X-692-70-164
PREPRINT

NASA TM X- 63910

CONFIGURATION OF THE GEOMAGNETIC TAIL DURING SUBSTORMS

D. H. FAIRFIELD
N. F. NESS

MAY 1970

GSFC — GODDARD SPACE FLIGHT CENTER
GREENBELT, MARYLAND

X-692-70164

CONFIGURATION OF THE GEOMAGNETIC TAIL DURING SUBSTORMS

D. H. Fairfield
N. F. Ness

Laboratory for Extraterrestrial Physics
NASA-Goddard Space Flight Center
Greenbelt, Maryland

May 1970

Space Plasma Physics Branch Preprint Series

1. Introduction

Magnetic field studies of the cislunar geomagnetic tail have determined the predominately solar anti-solar direction of the field (Ness, 1965), the dependence of the average field magnitude on the radial distance from the earth (Behannon, 1968; Mihalov et al., 1968; Mihalov and Sonett, 1968) and from the solar magnetospheric plane (Behannon, 1970. In addition, the component of the field perpendicular to the solar magnetospheric equatorial plane has been shown to be northward most of the time but southward occasionally (Mihalov et al., 1968; Behannon, 1970). On one unique occasion the field briefly had a component 30γ southward at 13 R_E near the center of the tail (Laird, 1969). Statistical studies have shown that the tail field tends to be large during times of high Kp (Behannon and Ness, 1966; Mihalov et al., 1968) and there is further evidence from particle and field measurements that the total flux in the tail increases during magnetic storms (Ness and Williams, 1966; Williams and Ness, 1966; Sugiura et al., 1968). Measurements in the tail (Heppner et al., 1967; Sugiura 1968) and at 6.6 R_E (Cummings and Coleman, 1968) have been compared to auroral zone magnetograms yielding correlations which suggest important changes in the tail field configuration during magnetospheric substorms.

The present paper extends the observations of tail-ground correlations and discusses their significance in relation to the wide range of substorm effects that have been observed on the ground and by spacecraft. Vector magnetic field measurements from the IMP 4 spacecraft (see Fairfield, 1969 for instrumental details) have been compared to the AE index of auroral zone ground magnetic activity (Davis and Sugiura, 1966) on 15 orbits during the interval February 5-April 15, 1968. The IMP 4 spacecraft is in an eccentric polar orbit with period of 4.3 days and apogee near the ecliptic plane. Each orbit is approximately confined to a meridian plane with the spacecraft outbound in the southern hemisphere and inbound in the northern hemisphere with neutral sheet crossings occurring beyond 25 R_E.

Section 2 develops a formula which is used in the remainder of the paper for predicting the location of the neutral sheet. Section 3 statistically examines a large data set to define the average dependence of the tail field on spatial coordinates and ground activity. Section 4 describes the direct comparison of the tail data and ground magnetic activity. Section 5 relates the magnetic field measurements to other measurements and to theories of substorms.

Results support the concept of an expanding plasma sheet during magnetospheric substorms. The field configuration after substorms has more lines of force crossing the equatorial plane within 30 R_E and thus supports the theory of field reconnection. The tail field morphology and the trapped particles bouncing on newly existing field lines agree with many other substorm observations. Extremely quiet geomagnetic conditions also correspond to a field configuration with more field lines crossing the equatorial plane in the cislunar tail region.

2. Location of the Neutral Sheet

In the initial phase of this tail study a method of predicting the position of the tail neutral sheet was developed and the accuracy of the prediction assessed. Although the $Z_{sm} = 0$ plane of solar magnetospheric coordinates (X_{sm} axis along the earth sun line, Z_{sm} axis in the plane formed by the dipole axis and the X_{sm} axis, and Y_{sm} completing a right handed orthogonal system) is expected to be a reasonable approximation of the location of the neutral sheet, it does not consider the tip of the dipole toward or away from the solar direction whose effect is to raise or lower the neutral sheet relative to the solar magnetospheric equatorial plane Murayama (1966) suggested that the neutral sheet could be approximated by a plane parallel to the solar magnetospheric equatorial plane and attached to the geomagnetic equatorial plane 8 R_E from the earth. Speiser and Ness (1967) studied the IMP 1 neutral sheet crossings and found that 10 R_E was a more suitable distance for attaching the neutral sheet. This plane can be represented by the formula

$$Z_{sn} = 10 \sin \chi_{ss} \tag{1}$$

where χ_{ss} is the geomagnetic latitude of the sun and Z_{sn} is in units of earth radii.

Russell and Brody (1967) extended the ideas of Murayama and suggested that since the neutral sheet was rooted near the geomagnetic equatorial plane which intersects the solar magnetospheric equatorial plane in the dawn-dusk meridian plane, the neutral sheet surface should be a curved surface part of a cylinder with axis parallel to the solar magnetospheric X axis). They used the position of IMP 1 and OGO 1 neutral sheet crossings to choose the appropriate constant and suggested the formula

$$Z_{RB} = (11^2 - Y_{sm}^2)^{\frac{1}{2}} \sin\chi_{ss} \text{ for } |Y_{sm}| \leq 11\ R_E \qquad (2)$$

In an attempt to extend this work additional neutral sheet crossing locations were determined from the tail data of IMP'S 2, 3 and 4. Most of the IMP 3 and 4 crossings were from greater radial distances than the IMP 1 and OGO-1 crossings and they exhibited greater scatter when located on a $\frac{Z_{sm}}{\sin\chi_{ss}}$ vs. Y_{sm} plot (Figure 1 of Russell and Brody). In spite of the greater scatter the location of the points suggested that the 11 R_E circle of the earlier work might be generalized to an ellipse. The formula

$$Z_F = (11^2 - \frac{11^2}{15^2} Y_{sm}^2)^{\frac{1}{2}} \sin\chi_{ss} \text{ for } |Y_{sm}| \leq 15\ R_E \qquad (3)$$

was finally selected as the prediction of the neutral sheet position. It is felt that this formula represents a slight, but not very significant, improvement over that of Russell and Brody at least for the IMP 4 crossing distances within 33 R_E. As pointed out by Russell and Brody, an improved relationship probably ought to depend on X_{sm} as well as Y_{sm}. Because of the anomalous but real variations in the position of the neutral sheet, further attempts to refine such prediction formulas will undoubtedly be difficult and of limited value.

Some measurement of the adequacy of the above prediction formula of equation 3 can be evaluated with the aid of Figure 1. Here the trajectory of IMP 4 projected in the plane perpendicular to the X axis has been plotted when it is in the region beyond $X_{sm} = -25\ R_E$. The top panels represent periods when the spacecraft was in the northern half of the tail which is characterized by solar directed fields and the bottom panels represent periods in the southern half ofthe tail with anti-solar directed fields. The vertical axes are solar ecliptic Z, solar magnetospheric Z and Z', where Z' is defined as the distance from the satellite to the predicted neutral sheet

$$Z' = Z_{sm} - Z_F = Z_{sm} - (11^2 - \frac{11^2}{15^2} = Y_{sm}^2)^{\frac{1}{2}} \sin\chi_{ss}. \qquad (4)$$

where Y_{sm} and Z_{sm} are the solar magnetospheric position coordinates of the spacecraft.

The gap in the center of the tail is due to the temporary 11 day failure of the spacecraft sun sensor which precluded a determination of the magnetic field direction. The solar ecliptic equatorial plane is obviously inadequate as an approximate location of the neutral sheet; the solar magnetospheric Z = 0 plane is a considerable improvement and Z' is an improvement over Z_{sm}. Although the Z' formula appears to give an adequate prediction for the location of the primary point of division for the two lobes of the tail, there are numerous brief intervals of opposite polarity occurring 5 R_E or more from Z' = 0. These brief occurrences of the opposite polarity are typically of the order of 10 minutes in length. From existing data it is not clear whether they represent large amplitude motion of the neutral sheet or more local perturbations. Since the tail field may sometimes have a substantial component in the northward direction as will be demonstrated in Sections 3 and 4, the reversals in question are not necessarily all 180° field reversals.

Z' will be assumed to be the distance between the spacecraft and the neutral sheet in the remainder of this paper.

3. Statistical Study of the IMP 4 Tail Data

The IMP 4 tail measurements made every 2.56 seconds were studied statistically by taking 2.5 minute averages of the field magnitude and the 3 solar magnetospheric components for all intervals when IMP F was beyond X= - 25 R_E on orbits 60-76. Examination of 20 second average plots confirmed that the spacecraft was always within the tail on these orbits. This data set consisted of 702.6 hours with the spacecraft between X_{se} = - 25 and X_{se} = - 33 R_E. Distributions of relevant quantities are presented in Figures 2-5.

Figure 2 shows the occurrence frequency of various strength fields for 2 R_E intervals of distance from the estimated position of the neutral sheet. The vertical arrows designate average values for the various Z' regions. The radial variation of the average field magnitude in this region is less than 3γ (Behannon, 1968; Mihalov et al., 1968) so most of the spread in the distribution is due to time variations. Low values centered near Z' = 0 confirm the observation of Behannon (1970) that a weak field region of width approximately that of the plasma sheet (Bame et al., 1967) surrounds the neutral sheet.

Figure 3 presents a similar distribution to that of Figure 2 only for the solar magnetospheric Z component of the field. This figure confirms previous observations that the northward (positive) Z_{sm} fields are considerably more frequent than southward fields. If fields with $|Z_{sm}| < 1\gamma$ are neglected as being essentially parallel to the solar magnetospheric plane, 2.5 minute average northward fields occur more frequently than southward fields in the ratio 6.5:1. This ratio is approximately that reported by Mihalov et al. (1968) for several Explorer 33 orbits at primarily greater distances. If fields with $|Z_{sm}| < 5\gamma$ are neglected this ratio increases to 20.4:1. Noteworthy in Figure 3 is the lack of any apparent dependence of the Z_{sm} component on distance from the neutral sheet. This will be important in Section 4 where it will be suggested that the component of the field across the neutral sheet can be deduced from measurements away from the neutral sheet. This lack of dependence on the Z_{sm} component on distance from the neutral sheet suggests that the tendency toward more northward fields near the neutral sheet (Behannon, 1970) is due to a Z'-independent positive Z_{sm} component being associated with reduced X_{sm} and Y_{sm} components in the region near the neutral sheet.

Figures 4 and 5 represent distributions illustrating the F and Z_{sm} dependence on geomagnetic activity. The solid trace in Figure 4 shows the magnitude distribution for all geomagnetic conditions while the dashed trace represents only 8.4% of the complete data set when the 2.5 minute AE value associated with each measurement is less than 20γ (20 is very near the noise level of the AE index and represents essentially no auroral zone magnetic activity). The tendency toward weaker fields during quiet times is in agreement with the findings of Behannon and Ness (1966) and Mihalov et al., (1968). No tail fields greater than 24 γ occur during these very quiet times.

Figure 5 represents the distribution of Z_{sm} using the same data sets as in Figure 4. The interesting difference is that the average Z_{sm} field during quiet times is 2.8 compared to only 1.8 for all geomagnetic conditions. Z_{sm} components greater than 5 are about twice as likely to occur during very quiet times. This result suggests that more than the average number of field lines cross the equatorial plane during quiet periods leaving less flux in the extended geomagnetic tail. This will be discussed in more detail in the next section.

4. Tail Morphology During Substorms

Although statistical studies such as that of Section 3 can summarize large quantitites of data and suggest gross effects concerning the relationship between the magnetic tail and ground activity, it is necessary to examine the relevant parameters as a function of time to fully appreciate their relationship. For this purpose the 20 second averages of the IMP 4 tail field magnitude F, solar magnetospheric Z component Z_{sm}, latitude angle θ, and longitude φ were plotted along with the 2.5 minute values of the AE index which is a measurement of auroral zone magnetic activity. The AE index was compiled by superposing magnetograms from the auroral zone stations - College, Sitka, Meanook, Great Whale River and Leirvogur. Lack of data from the Soviet Union means that substorms during the universal time interval 1700-2200 are often not adequately detected. Representative examples are presented in Figures 6-10.

Figure 6 illustrates the typical behavior of the geomagnetic tail during clearly defined isolated substorms. Before the substorm and during its early phases the magnitude of the field increases but the Z_{sm} component remains small (3:00-4:30 and 6:30-7:50). At a time which is usually near the maximum of the substorm, the field decreases over a time interval which is either of order ten minutes (4:20 in Figure 6) or more abruptly (7:50). Accompanying or shortly following this decrease in field magnitude is an increase in the Z_{sm} component of the field. When the spacecraft is within a few earth radii of the neutral sheet (Z' small) the F decrease is often large enough such that the Z_{sm} component approaches the total field magnitude and the field points north (4:40-5:40 and 8:15-9:30).

This decreasing field morphology corresponds closely to the morphology for arrival of enhanced plasma and particles associated with an expanding plasma sheet (Hones et al., 1967, Rothwell and Wallington, 1968; Meng and Anderson, 1970) and it is natural to associate the two. This type of behavior where the field decreases and the plasma increases while the total energy density remains constant has previously been reported for one event (Lazarus et al., 1968). Two contrasting states of the neutral sheet are illustrated by comparing the crossing (Ø angle reversal) near 5:20 where the field is northward after the substorm with the brief crossings near 7:10 which are rapid and have little northward flux. The concept of an expanding and contracting weak field region is also supported by the statistical study of Figure 4 in which the broadest distribution of F occur in the region from 1 to 5 R_E from the neutral sheet.

An example of substorm morphology when the spacecraft is farther from the neutral sheet is presented in Figure 7. Again the field magnitudes increase prior to and during the early phases of the substorms which peak near 12:45 and 16:45. The decreasing fields beginning near the substorm maxima are more gradual and probably do not correspond to the appearance of the plasma sheet. The further F decrease at 18:15, however, probably corresponds to the arrival of the plasma sheet despite the fact that the spacecraft is predicted to be almost 9 R_E from the neutral sheet. The usual Z_{sm} increases can be seen beginning shortly after the substorm maximum.

Although previous work investigating the field across the neutral sheet has involved looking at detailed measurements at the time of the crossing, the IMP 4 data suggests that similar information can be obtained farther from the neutral sheet. This is reasonable when one considers that field lines are continuous and the flux crossing the equatorial plane must be closely related to that crossing a parallel plane somewhat displaced from the equatorial plane. Although changes in the orientation of the tail due to solar wind direction changes can certainly produce appreciable changes in the Z_{sm} component at any instant of time (Speiser and Ness, 1967) they certainly do not obscure the tendency for Z_{sm} to increase after substorms. This observed Z_{sm} increase cannot be related to tail tipping since the northward increase is observed in both northern and southern hemispheres during virtually every well-defined substorm; whereas, tipping the tail will produce a southward change of Z_{sm} in one hemisphere or the other.

Although substorms represent an important and dramatic component of auroral zone magnetic activity, they are seldom as isolated and well-defined as those of Figures 6 and 7. Figure 8 illustrates a 7-hour period on March 2-3, 1968 when moderate auroral zone activity is present but substorms are not in evidence. Typical of these periods is a substantial but variable northward Z_{sm} component. Since the spacecraft is near the neutral sheet region in Figure 8 the field is weak and directed quite northward. Although one might define the φ change at 1:02 as the neutral sheet it is clear that the field is substantially northward throughout this interval and it is only a relatively small XY field component which is controlling the φ angle. With this type of data the selection of neutral sheet crossings is not straightforward which accounts for some of the difficulties in pursuing work like that of Section 2.

The tail during a large disturbance is illustrated in Figure 9 (note the change in scales). Again during a sustained period of high latitude ground activity there is a strong northward Z_{sm} component throughout most of the interval. The short southward excursions of Z_{sm} (3:35, 4:40, 6:30 and 8:45) are not uncommon, particulary during disturbed periods, but their morphology has not been determined.

Figure 10 represents a relatively quiet interval and illustrates how even very small ground disturbances are associated with increasing F and small Z_{sm}. In spite of the very weak fields near 14:30 and 18:00 the average Z_{sm} during these times is greater than that during the disturbed period from 15:30-17:00.

Figure 11 presents data from an extended period of 19 hours on February 14-15, 1968 which is unique because of the total lack of auroral zone ground activity for the extended period which ends about 21:00. The field data are also unique in that the average Z_{sm} component of field strength is about 7γ for this period at a spacecraft position near apogee more than 33 R_E from the earth and at $|Z'| < 5$ R_E and $Y_{sm} \approx -12$ R_E. Although part of this large Z_{sm} component could reflect a tendency for northward field at large $|Y_{sm}|$, enhanced Z_{sm} components are also seen nearer the tail axis. Apparently during this extended quiet period the field was able to relax to a more dipolar state with more gradual field line curvature and more flux crossing the equatorial plane.

The very quiet period on February 14 is even more unique because of the occurrence of a small storm sudden commencement at 12:53 on this day which was followed by only the smallest hint of a main phase type decrease at a few observatories. Explorer 33 in the interplanetary medium measured an abrupt increase from 8 to 11γ which is typically associated with the sudden commencements (Taylor, 1968) and the field remained near 12γ during the succeeding 12 hours. Of apparent importance was the northward-pointing character of the interplanetary field which persisted until 21:00 when the first southward excursion of the period occurred at the time of the buildup in tail field magnitude and AE. Moderate disturbance at the polar cap stations Resolute Bay and Mould Bay did begin as early as 14:00.

5. Discussion

The results of Section 4 indicate that the configuration of the geomagnetic tail changes during substorms with the primary effect being that additional lines of force cross the equatorial plane in the inner tail region after the substorms. This supports the reconnection theories (Dungey, 1968; 1968b, Axford, 1967; Piddington, 1968a, 1968b; Atkinson, 1966), whereby field lines going far into the tail or off into interplanetary space are converted into closed geomagnetic field lines. The results do not prove reconnection since it is possible that field lines that crossed the neutral sheet far back in the tail before the substorm simply contract until they have their crossing points much nearer the earth. In either case, the magnetic tail is in a lower energy state after the substorm and the results strongly suggest that energy is stored in the tail until its release during the substorm (Atkinson, 1966; Siscoe and Cummings, 1969). The contraction of previously extended field lines is probably a factor in the production of energetic particles associated with the substorms. Two configurations of the geomagnetic tail are depicted in Figures 12 and 13 which illustrate the narrow plasma sheet with little flux crossing the equatorial plane appropriate to conditions just before a substorm (Figure 12) and the expanded plasma sheet with enhanced flux crossing the equatorial plane appropriate to conditions after the substorm or during quiet conditions (Figure 13).

The creation of additional field lines crossing near the earth has several consequences which help to explain other measurements. The increase in Z_{sm} is consistent with an expanding field-aligned plasma sheet as has been suggested by Hones et al. (1967, 1968, 1970), Hones (1969), Rothwell and Wallington (1968) and Meng and Anderson (1970). Energetic particles are able to exhibit bounce motion on the newly created field lines. As more closed lines are formed, the region of closed lines expands explaining the appearance of energetic particles near 18 R_E, the "electron islands" further back in the tail (Anderson, 1965; Anderson and Ness, 1966; Meng and Anderson, 1970) and the poleward motion of trapped particle boundaries which are observed to increase their latitude to at least 76° after substorms (Rao, 1969; Lin et al., 1968; Fritz, 1968, 1970). Fritz (1968) speculated that the field did not control the high latitude cutoff of trapped particles since he found the boundary could vary on relatively quiet days but the example of Figure 10 shows that the tail can change its configuration even in association with very small disturbances.

The poleward expansion of the auroral arcs and the equatorial electrojet during substorms (Akasofu et al., 1966) and the riometer absorption region (Jelly and Brice, 1967; Jelly, 1968) are other observations consistent with the magnetic field behavior. In this connection it is attractive to associate the northern boundary of aurora with the outer edge of the plasma sheet and the last closed field line as suggested by Vasyliunas (1969).

The equatorial crossing points of field lines can be estimated by extending the flux conservation analysis (Fairfield, 1968) to these quiet and post-substorm periods. In the earlier analysis for an average magnetosphere it was assumed that the component of flux across the equatorial plane in the midnight meridian decreased to 5γ at 15 R_E in a manner such that the field line from 69° latitude crossed the equatorial plane near 15 R_E. Results of Section 4 now indicate that normal components of 7γ are not unreasonable at distances as great as 33 R_E at certain times.

In extending this analysis let us assume that the flux from the 15° longitude region near midnight is confined to a longitude section such that field lines cross the equatorial plane within 1.5 R_E of the noon midnight meridian plane. If a constant normal field of 7γ is assumed between 15 and 35 R_E, the field lines from 70°, 72° and 74° latitutde are calculated to cross the equatorial plane near 20 R_E, 28 R_E and 36 R_E. Obviously these particular numbers are subject to uncertainties and are sensitive to Z_{sm} and its radial variation but they are indicative of the type of field lines one can expect to find after substorms and during quiet times when enhanced flux crosses the equatorial plane.

It is of further interest to estimate the affects of the changing configuration on the extended geomagnetic tail. Fairfield (1968) determined that 7100γ R_E^2 of flux cross a plane perpendicular to the X_{sm} axis at 15 R_E and go into one quarter of an approximately circular tail. If the area of half the equatorial plane in the tail between 15 and 35 R_E is taken as 20 R_E x 18 R_E = 360 R_E^2 and the normal field strength as 7γ, then 2520γ R_E^2 of flux will cross the equatorial plane and be lost to the downstream tail. This is 35% of the flux entering the tail at 15 R_E. Although part of the flux entering the tail at 15 R_E crosses the equatorial plane even during average conditions it is apparent that the flux crossing the tail during extreme conditions represents an appreciable fraction of that which would go far back into the tail at most other times. If one considers additional field lines closing beyond the apogee of IMP 4, it is not unreasonable to suggest that at the orbit of the moon (60 R_E) half the average flux in the tail might disappear at certain times.

Summary

The following phenomenological description for the processes occurring in the magnetic tail during magnetospheric substorms contains the ideas of many authors and will serve to summarize the results of this paper and their relation to other existing work. Association of the plasma sheet with the auroral oval is a primary assumption in relating low altitude events to those of the tail.

Conditions in the solar wind such as the occurrence of strong and southward directed interplanetary fields (see summary by Hirshberg and Colburn, 1969) sets into motion or enhances the interaction mechanism between the solar wind and the magnetosphere. Dayside field reconnection is a likely mechanism but not necessarily the only possible one. This increased interaction rate forces additional field lines into the geomagnetic tail. Since the tail field magnitude is controlled by magnetosheath plasma pressure acting on the tail boundary the simple process of adding field lines to the tail does not increase the tail field strength. Adding flux to the tail does, however, increase the geometrical cross section of the tail producing more flaring of the boundary and subjecting it to a larger component of pressure from the solar plasma flowing in the magnetosheath. In this manner an enhanced pressure produces the increase in the tail field observed before and during the early phases of a substorm (Lazarus et al., 1968). Increase in the ambient solar wind pressure could also produce the observed increase but such an association between plasma parameters and substorms is not apparent in data reported to date (Gosling et al., 1967). In this manner energy is stored in the geomagnetic tail and conditions are set for a substorm (Siscoe and Cummings, 1969). At this point prior to the explosive beginning of a substorm the neutral and plasma sheets attain their minimum thicknesses, relatively little flux crosses the equatorial plane between 10 R_E and 35 R_E, and a maximum of flux goes into the tail as depicted in Figure 12.

First observable effects of the explosive phase of the substorm seem to be located on field lines associated with the low latitude edge of the auroral oval (inner edge of the plasma sheet). Frequently brightening of the most equatorward auroral arc (Akasofu, 1964) is the first visual indication of an imminent substorm. A prompt increase in energetic particles and magnetic field at 6.6 R_E near midnight is observed coincident with the sudden increase in auroral zone magnetic activity which is often considered the beginning of the substorm. It seems unlikely that the neutral sheet (outer edge of the plasma sheet) is involved in initiating the substorm unless somehow information is transmitted through the plasma sheet without disrupting the field lines supporting quiet arcs.

As the substorm progresses the plasma sheet expands accounting for the post substorm arrival of plasma and energetic particles at spacecraft in the inner tail region and the appearance of the neutral sheet-related weak field region at IMP 4. Associated with this expanded sheet are an increased number of tail magnetic field lines crossing the equatorial plane in cislunar space (Figure 13). These newly existing field lines are responsible for the increased Z_{sm} at IMP 4 and allow bouncing particles to exist at latitudes at least as high as 76° (Rao, 1969; Lin et al., 1968; and Fritz 1968, 1970). Since the outer boundary of the plasma sheet and the outermost closed field line are still associated with the auroral oval, the creation of additional closed field lines corresponds to the poleward motion of auroral arcs and the associated auroral electrojet and particle precipitation regions. The inward motion of the inner edge of the plasma sheet is associated with the southward expansion of the auroral region. The reduction of flux in the tail as more field lines become closed near the earth reduces the cross-sectional area of the tail, decreases the magnetosheath pressure on the tail, and accounts for the decrease in tail field strength away from the neutral sheet. Although reduction of total pressure cannot be inferred from the magnetic field data alone, the similarity of the Pioneer 7 event discussed by Lazarus et al. (1968) suggests that such may be the case. Other important processes which could be associated with the earthward motion of field lines involve particle acceleration and the generation of magnetospheric currents (Axford, 1969; Vasyliunas, 1970; Taylor, 1970).

In the complete absence of substorms the magnetosphere appears to remain in a state similar to that attained after substorms with much flux crossing the equatorial plane at cislunar distances. The association of the outer boundary of closed field lines with the northern edge of the auroral oval is supported by the results of Stringer and Belon (1967) who show that for Kp = 0 the occurrence of aurora maximizes at latitudes above 70°.

Acknowledgements

The authors wish to thank Mr. J. B. Seek who carried out the instrumentation and testing of the IMP 4 magnetic field experiment.

[redacted]

REFERENCES

Akasofu, S. I., The Development of the Auroral Substorm, Planet Space Sci., 12, 273-282, 1964.

Akasofu, S-I., D. S. Kimball and C. I. Meng, Dynamics of the Aurora V: Poleward Motions, J. Atmospheric Terrest. Phys., 28, 497-503, 1966.

Anderson, K. A., Energetic Electron Fluxes in the Tail of the Geomagnetic Field, J. Geophys. Res., 70, 4741-4764, 1965.

Anderson, K. A. and N. F. Ness, Correlation of Magnetic Fields and Energetic Electrons in the IMP 1 Satellite, J. Geophys. Res., 71, 3705-3727, 1966.

Atkinson G., A Theory of Polar Substorms, J. Geophys. Res., 71, 5157-5164, 1966.

Axford, W. I., Magnetospheric Convection, Reviews of Geophysics, 7, 421-459, 1969.

Axford, W. I., Magnetic Storm Effects Associated with the Tail of the Magnetosphere, Space Sci. Rev., 7, 149-157, 1967.

Bame, S. J., J. R. Asbridge, H. E. Felthauser, E. W. Hones, and I. B. Strong, Characteristics of the Plasma Sheet in the Earth's Magnetotail., J. Geophys. Res., 72, 113-129, 1967.

Behannon, Kenneth W., Mapping of the Earth's Bow Shock and Magnetic Tail by Explorer 33, J. Geophys. Res., 73, 907-930, 1968.

Behannon, Kenneth W., Geometry of the Geomagnetic Tail, J. Geophys. Res., 75, 743-753, 1970.

Behannon, K. W. and N. F. Ness, Magnetic Storms in the Earth's Magnetic Tail, J. Geophys. Res., 71, 2327-2351, 1966.

Cummings, W. D., and P. J. Coleman, Jr., Simultaneous Magnetic Field Variations at the Earth's Surface and at Synchronous, Equatorial Distance. Part 1. Bay Associated Events, Radio Sci., 3, 758-761, 1968.

Davis, T. Neil, and Masahisa Sugiura, Auroral Electrojet Activity Index AE and Its Universal Time Variations, J. Geophys. Res., 71, 785-801, 1966.

Dungey, J. W., The Reconnection Model of the Magnetosphere in The Earth's Particles and Fields, edited by B. M. McCorma, p. 385-392, Reinhold Publishing Corp., New York 1968.

Dungey, J. W., Polar Substorms: Theoretical Review, Space Research 8, edited by A. P. Mitra, L. G. Jacchia, and W. S. Newman, pp. 243-252, North Holland Publishing Corp., Amsterdam, 1968b.

Fairfield, D. H., Average Magnetic Field Configuration of the Outer Magnetosphere, J. Geophys. Res., 73, 7329-7338, 1968.

Fairfield, D. H., Bow Shock Associated Waves Observed in the Far Upstream Interplanetary Medium, J. Geophys. Res., 74, 3541-3553, 1969.

Fritz, Theodore A., High Latitude Outer-Zone Boundary Region for ≥ 40-kev Electrons During Geomagnetic Quiet Periods, J. Geophys. Res., 73, 7245-7255, 1968.

Fritz, Theodore A., High Latitude Outer Zone Boundary Region for ≥ 40 kev Electrons with Injun 3, Goddard Space Flight Center preprint X-646-70-70, 1970.

Gosling, J. T., J. R. Asbridge, S. J. Bame, A. J. Hundhausen, I. B. Strong, Measurements of the Interplanetary Solar Wind During the Large Geomagnetic Storm of April 17-18, 1965, J. Geophys. Res., 72, 1813, 1967.

Heppner, J. P., M. Sugiura, T. L. Skillman, B. G. Ledley and M. Campbell, OGO-A Magnetic Field Observations, J. Geophys. Res., 72, 5417-5471, 1967.

Hirshberg, J. and D. S. Colburn, Interplanetary Field and Geomagnetic Variations - A Unified View, Planet. and Space Sci., 17, 1183-1206, 1969.

Hones, E. W., Jr., S. I. Akasofu, P. Perrault, S. J. Bame, and Sidney Singer, Poleward Expansion of the Auroral Oval and Associated Phenomena in the Magnetotail During Auroral Substorms (I), preprint March 1970.

Hones, E. W., Jr., Magnetotail Plasma and Magnetospheric Substorms, paper presented at the Summer Advanced Study Institute, Earth's Particles and Fields, Santa Barbara, California August 4-14, 1969.

Hones, E. W., Jr., J. R. Ashbridge, S. J. Bame and I. B. Strong, Outward Flow of Plasma in the Magnetotail Following Geomagnetic Bays, J. Geophys. Res., 72, 5879-5892, 1967.

Hones, E. W., Jr. and S. Singer and C. S. R. Rao, Simultaneous Observations of Electrons (E> 45 kev) and 2000 Kilometer Altitude and at 100,000 Kilometers in the Magnetotail, J. Geophys. Res., 73, 7339-7359, 1968.

Jelly, D. H., Apparent poleward Motion of Onsets of Auroral Absorption Events, Canad. J. Phys., 46, 33, 1968.

Jelly, D. H., and N. Brice, Changes in Van Allen Radiation Belt Associated with Polar Substorms, J. Geophys. Res., 72, 5919, 1967.

Laird, M. J., Structure of the Neutral Sheet in the Geomagnetic Tail, J. Geophys Res., 74, 133-139, 1969.

Lazarus, A. J., G. L. Siscoe and N. F. Ness, Plasma and Magnetic Field Observations During the Magnetosphere Passage of Pioneer 7, J. Geophys. Res., 73, 2399-2409, 1968.

Lin, W. C., I. B. McDiarmid and J. R. Burrows, Electron Fluxes at 1000 km Altitude Associated with Auroral Substorms, Can. J. Phys., 46, 80-83, 1968.

Meng, C. I. and K. A. Anderson, Space Sciences Laboratory, University of California, Berkeley Preprint, April 1970.

Mihalov, J. D. and C. P. Sonett, The Cislunar Geomagnetic Tail Gradient in 1967, J. Geophys. Res., 73, 6837-6841, 1968.

Mihalov, J. D., D. S. Colburn, R. G. Currie, and C. P. Sonett, Configuration and Reconnection of the Geomagnetic Tail, J. Geophys. Res., 73, 943-959, 1968.

Murayama, T., Spacial Distribution of Energetic Electrons in the Geomagnetic Tail, J. Geophys. Res., 71, 5547, 1966.

Ness, N. F., The Earth's Magnetic Tail, J. Geophys. Res., 70, 2989-3005, 1965.

Ness, N. F. and Williams, D. J., Correlated Magnetic Tail and Radiation Belt Observations, J. Geophys. Res., 71, 322-325, 1966.

Piddington, J. H., The Growth and Decay of the Geomagnetic Tail in Earth's Particles and Fields, edited by B. M. McCormac, pp. 417-427, Reinhold Publishing Co., New York 1968a.

Piddington, J. H., The Magnetospheric Radiation Belt and Tail Plasma Sheet, Planet. Space Sci., 16, 703-716, 1968b.

Rao, C. S. R, Some Observations of Energetic Electrons in the Outer Radiation Zone During Magnetic Bays, J. Geophys. Res., 74, 794-801, 1969.

Rothwell, P. and V. Wallington, The Polar Substorm and Electron 'Islands' in the Earth's Magnetic Tail, Planet. and Space Sci., 16, 1441-1451, 1968.

Russell, Christopher T., and Kenneth I. Brady, Some Remarks on the Position of the Neutral Sheet, J. Geophys. Res., 72, 6104-6106, 1967.

Siscoe, G. L. and W. D. Cummings, On the Cause of Geomagnetic Bays, Planet. Space Sci., 17, 1795-1802, 1969.

Speiser, T. W. and N. F. Ness, The Neutral Sheet in the Geomagnetic Tail; Its Motion, Equivalent Currents, and Field Line Reconnection Through It, J. Geophys. Res., 72, 131-141, 1967.

Stringer, W. J. and A. E. Belon, The Statistical Auroral Zone During IQSY and Its Relationship to Magnetic Activity, J. Geophys. Res., 72, 245-250, 1967.

Sugiura, M., T. L. Skillman, B. G. Ledley, and J. P. Heppner, Propagation of the Sudden Commencement of July 8, 1966, to the Magnetotail, J. Geophys., Res., 73, 6699-6709, 1968.

Sugiura, Masahisa, Results of Magnetic Surveys of the Magnetosphere and Adjacent Regions. Goddard Space Flight Center Preprint X-612-69-12. January 1969. Presented at the IAGA Symposium on Description of the Earth's Magnetic Field, Washington, D.C. October 1968; to be published in the Report of the World Magnetic Survey.

Taylor, H. E., Sudden Commencement Associated Discontinuities in the Interplanetary Magnetic Field Observed by IMP 3, Solar Physics, 6, 320, 1968.

Taylor, Harold E. and Francis W. Perkins, Auroral Phenomena Drive by the Magnetospheric Plasma, Preprint 1970.

Vasyliunas, Vytenis M., Mathematical Models of Magnetospheric Convection and Its Coupling to the Ionosphere, to be published in Particles and Fields in the Magnetosphere, edited by B. M. McCormac, D. Reidel Publishing Co., Dordrecht, Holland, 1970.

Vasyliunas, Vytenis M., Low Energy Particle Fluxes in the Geomagnetic Tail, to appear in Production and Maintenance of the Polar Ionosphere, edited by G. Skovli, 1969.

Williams, Donald J. and Norman F. Ness, Simultaneous Trapped Electron and Magnetic Tail Field Observations, J. Geophys. Res., 71, 5117-5128, 1966.

FIGURE CAPTIONS

Figure 1 IMP 4 trajectory plots for times when the spacecraft was beyond $X = -25\ R_E$ in the geomagnetic tail and the field was directed toward the earth (top) and away from the earth (bottom). In each block the trajectory is projected on the plane perpendicular to the earth-sun line in solar ecliptic coordinates, solar magnetospheric coordinates, and in a coordinate system where the vertical axis Z' takes into account the tip of the dipole toward or away from the sun.

Figure 2 Relative occurrence frequencies of 2.5 minute average tail field magnitudes at position $-25 > X_{SM} > -33\ R_E$ for 2 R_E intervals of distance from the expected position of the neutral sheet. The vectors denoting the average values for each 2 R_E interval have their lowest values in a region centered on the Z' = 0 position of the neutral sheet.

Figure 3 Relative occurrence frequencies of 2.5 minutes averages of the Z_{SM} component of the tail field for 2 R_E interval of distance from the expected position of the netural sheet. The vectors denoting the average in each 2 R_E region show an average northward component which exhibits no apparent variation with distance from the neutral sheet.

Figure 4 Relative occurrence frequency of IMP 4 tail magnitudes for all geomagnetic conditions (solid line) and for very quiet conditions (dashed line). Low field magnitudes tend to be associated with quiet conditions.

Figure 5 Relative occurrence frequency of the Z_{SM} component of the tail field for all geomagnetic conditions for very quiet conditions. Higher Z_{SM} components tend to be associated with quiet times.

Figure 6 Geomagnetic AE index, tail field magnitude F and solar magnetospheric field component Z_{SM}, latitude angle θ and longitude angle ϕ. Data are typical of that seen during isolated substorms when IMP 4 is in the vicinity of the neutral sheet. During the early phases of a substorm F increases and Z_{SM} becomes small, whereas during the later phases F decreases and Z_{SM} increases.

Figure 7 Behavior of the tail field during isolated substorms when the spacecraft is far from the expected position of the neutral sheet. The anti correlation of F and Z_{SM} is still apparent but the decrease in F is generally more gradual.

Figure 8 Observations of the tail field near the neutral sheet region at $X_{SM} = -33$ $Y_{SM} = -2$ during an extended period of moderate geomagnetic disturbance with no well defined substorms.

Figure 9 Observations of the tail field near the neutral sheet during a period of intense magnetic disturbance. The field is characterized by a large average northward component but includes several brief intervals of southward field.

Figure 10 Observations of the tail field during a period of moderate disturbance surrounded by quiet intervals. The Z_{SM} component is small and F is large during the disturbances but Z_{SM} is increased even though F is very small during the quiet periods.

Figure 11 Observation of a very northward field during an extended quiet interval at average position X = -31 R_E, Y = -12 R_E. The end of the geomagnetically quiet interval is associated with an increasing F and decreasing Z_{SM}.

Figure 12 Field configuration in the noon midnight meridian plane drawn to illustrate the thin plasma sheet and small Z_{SM} component associated with the early phases of a geomagnetic substorm.

Figure 13 Field configuration in the near midnight meridian plane drawn to illustrate an expanded plasma sheet with enhanced flux crossing the equatorial plane. This configuration exists during quiet conditions or following a substorm.

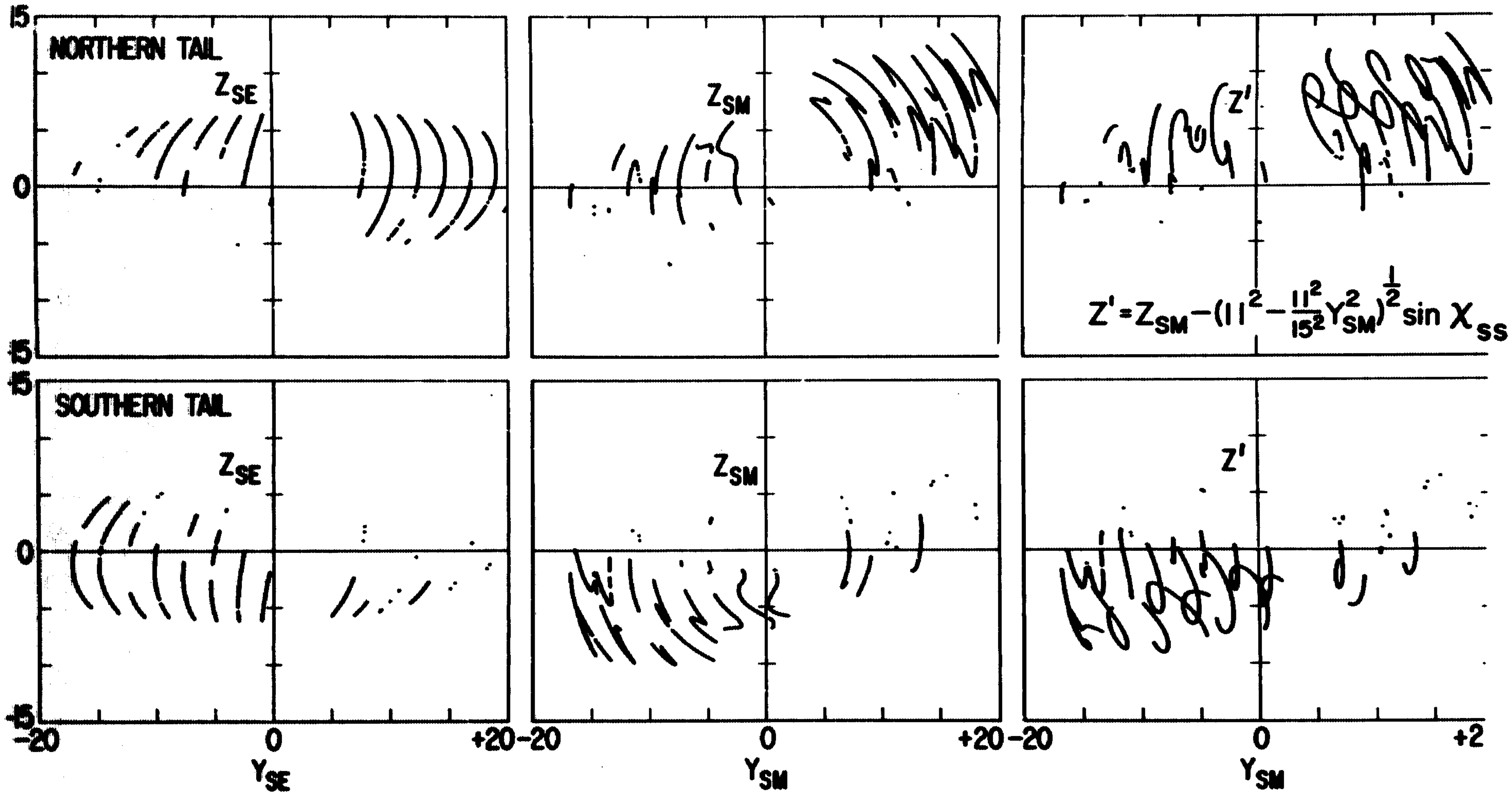

IMP-4 TAIL TRAJECTORY

FIGURE 1

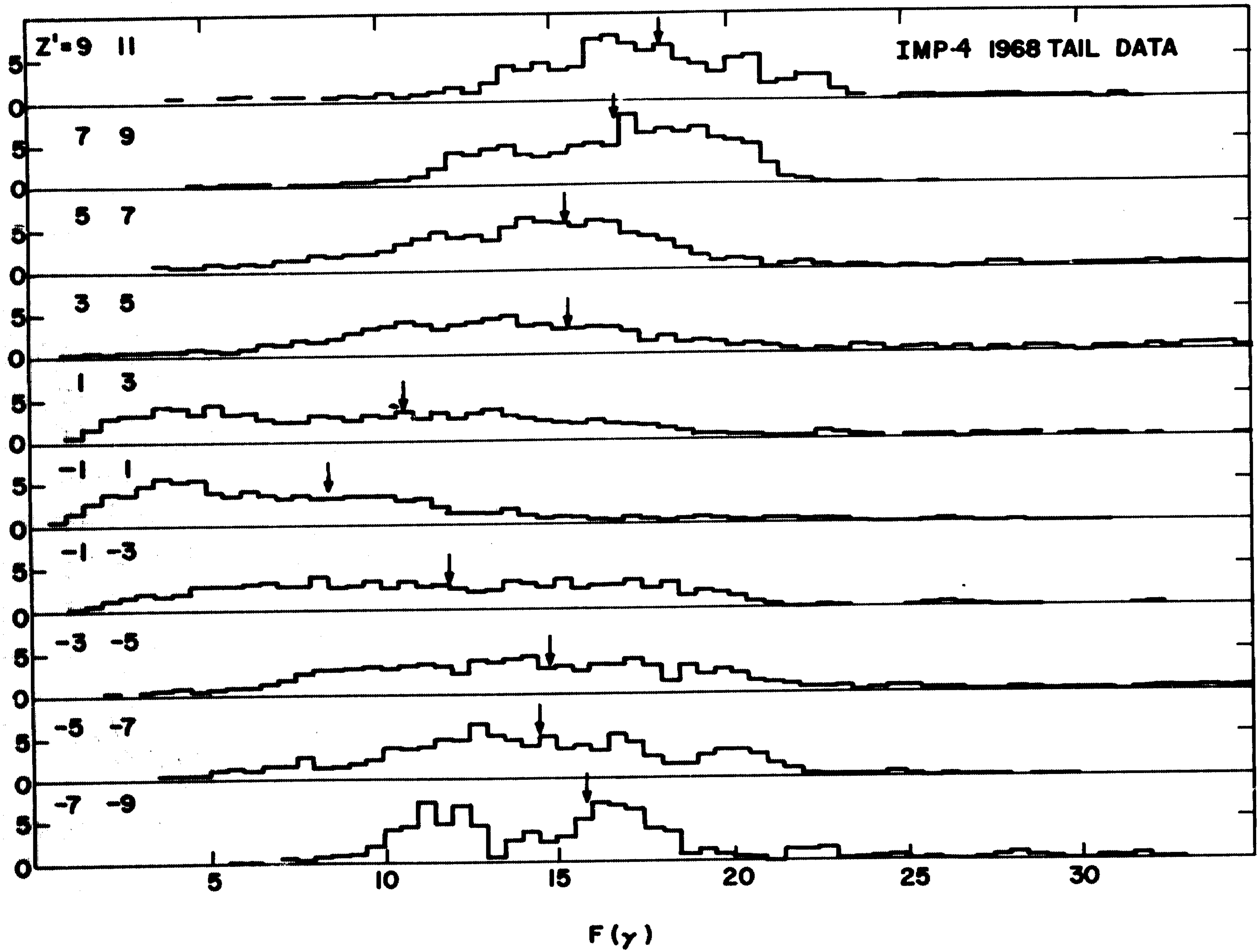
IMP-4 1968 TAIL DATA
Z'=9 11
7 9
5 7
3 5
1 3
-1 1
-1 -3
-3 -5
-5 -7
-7 -9
5
0
5
10
15
20
25
30
F(γ)

FIGURE 2

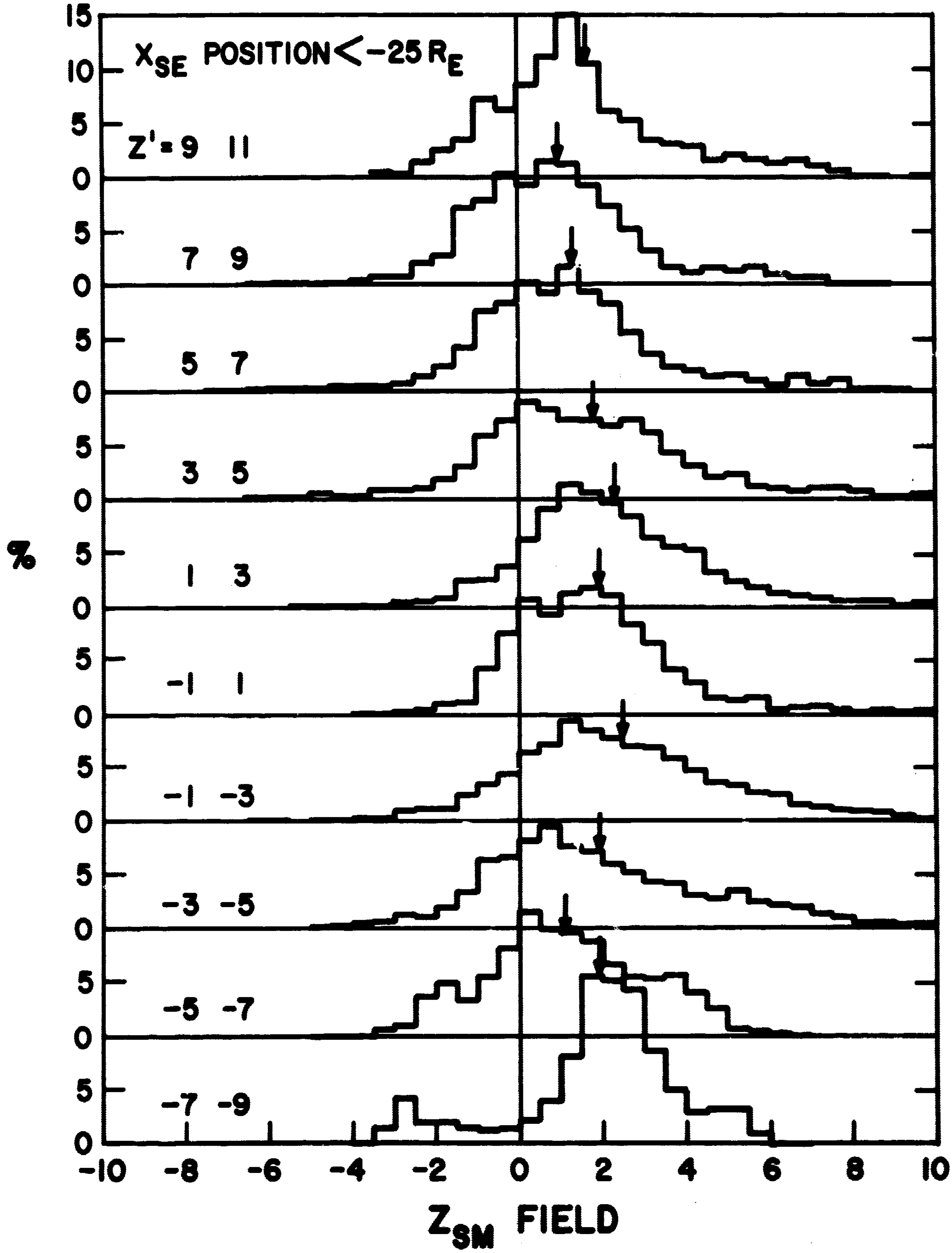

X_{SE} POSITION < -25 R_E
Z' = 9 11
7 9
5 7
3 5
1 3
-1 1
-1 -3
-3 -5
-5 -7
-7 -9
%
15
10
5
0
-10 -8 -6 -4 -2 0 2 4 6 8 10
Z_{SM} FIELD

FIGURE 3

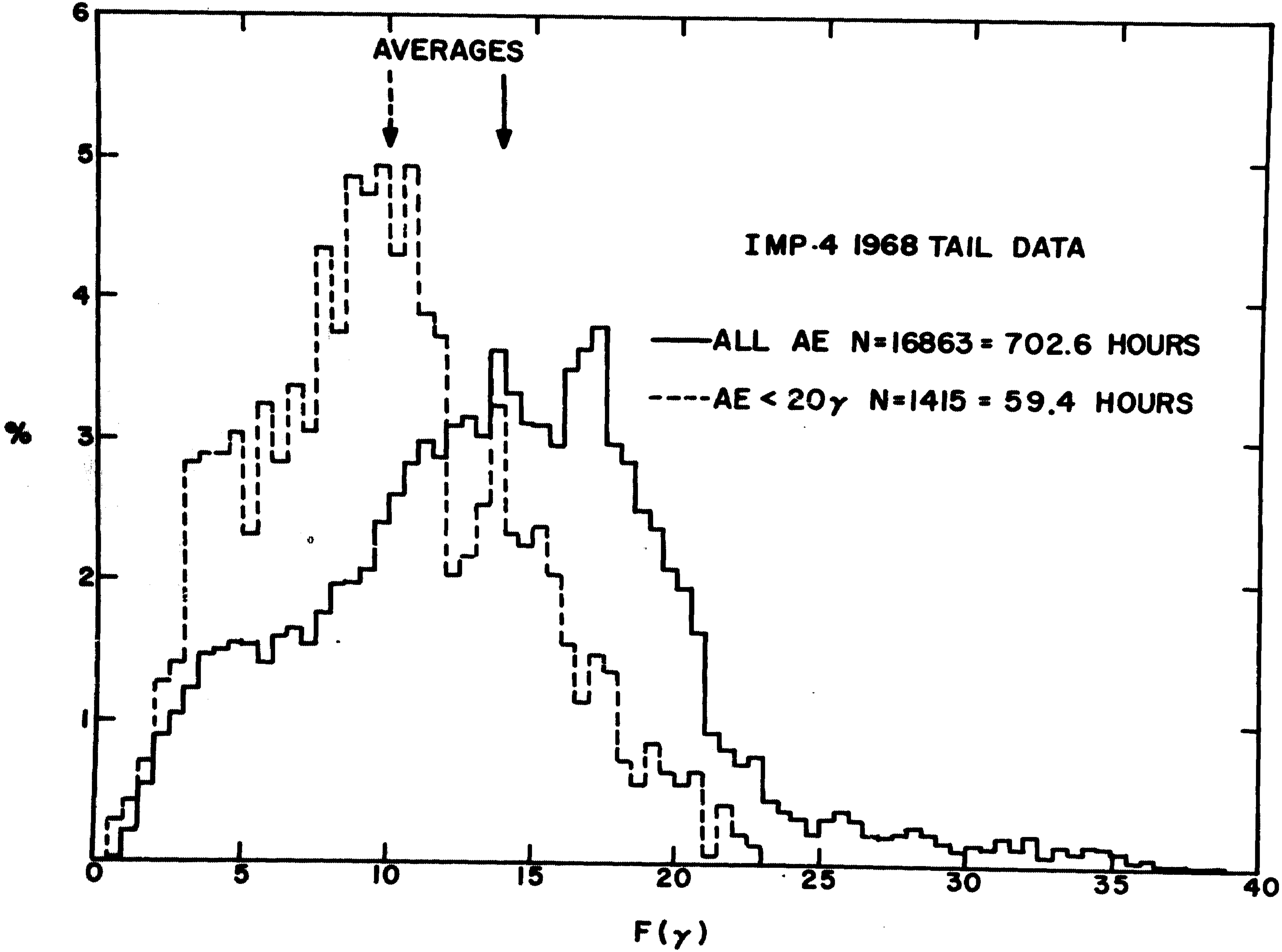
AVERAGES
IMP-4 1968 TAIL DATA
——ALL AE N=16863 = 702.6 HOURS
----AE < 20γ N=1415 = 59.4 HOURS
%
0
1
2
3
4
5
6
0
5
10
15
20
25
30
35
40
F(γ)

FIGURE 4

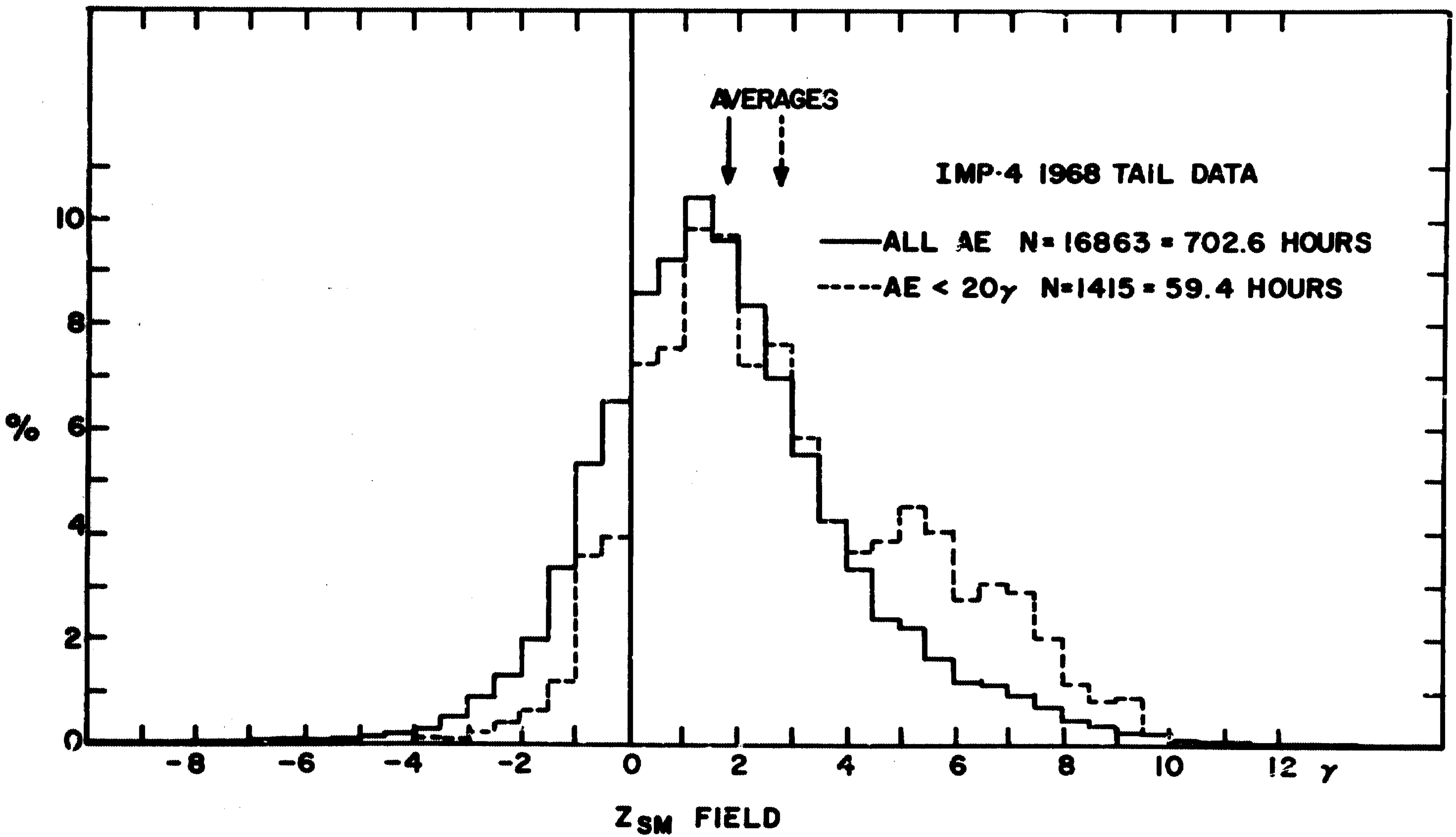
AVERAGES
IMP-4 1968 TAIL DATA
——ALL AE N = 16863 = 702.6 HOURS
-----AE < 20γ N = 1415 = 59.4 HOURS
%
10
8
6
4
2
0
-8
-6
-4
-2
0
2
4
6
8
10
12 γ
Z SM FIELD

FIGURE 5

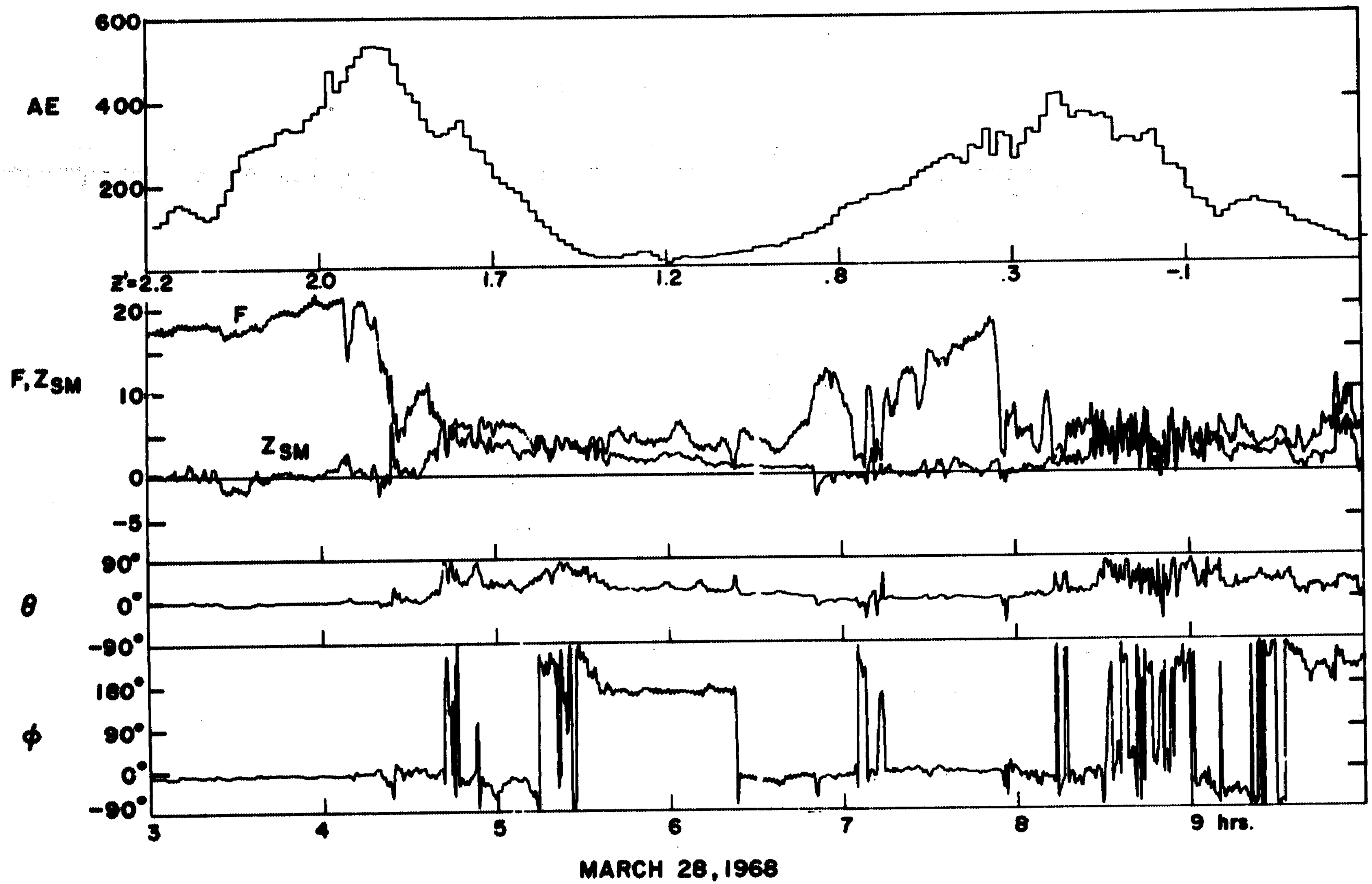
AE
600
400
200
Z'=2.2
2.0
1.7
1.2
.8
.3
-.1
F,Z_{SM}
F
Z_{SM}
20
10
0
-5
θ
90°
0°
-90°
φ
180°
90°
0°
-90°
3
4
5
6
7
8
9 hrs.
MARCH 28, 1968

FIGURE 6

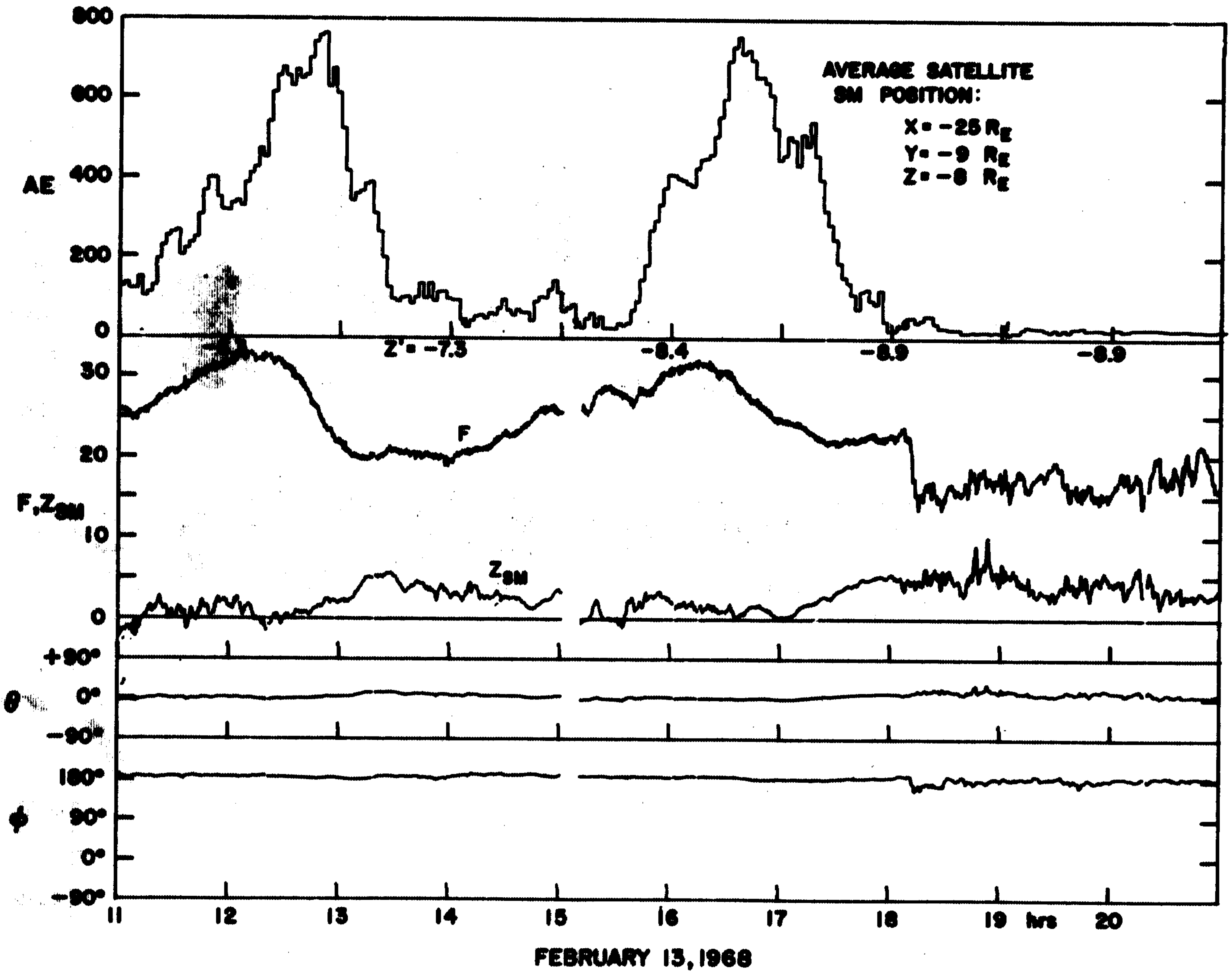
AE
800
600
400
200
0
AVERAGE SATELLITE
SM POSITION:
X = -25 R_E
Y = -9 R_E
Z = -8 R_E
Z' = -7.3
-8.4
-8.9
-8.9
F, Z_{SM}
30
20
10
0
F
Z_{SM}
θ
+90°
0°
-90°
φ
180°
90°
0°
-90°
11
12
13
14
15
16
17
18
19 hrs
20
FEBRUARY 13, 1968

FIGURE 7

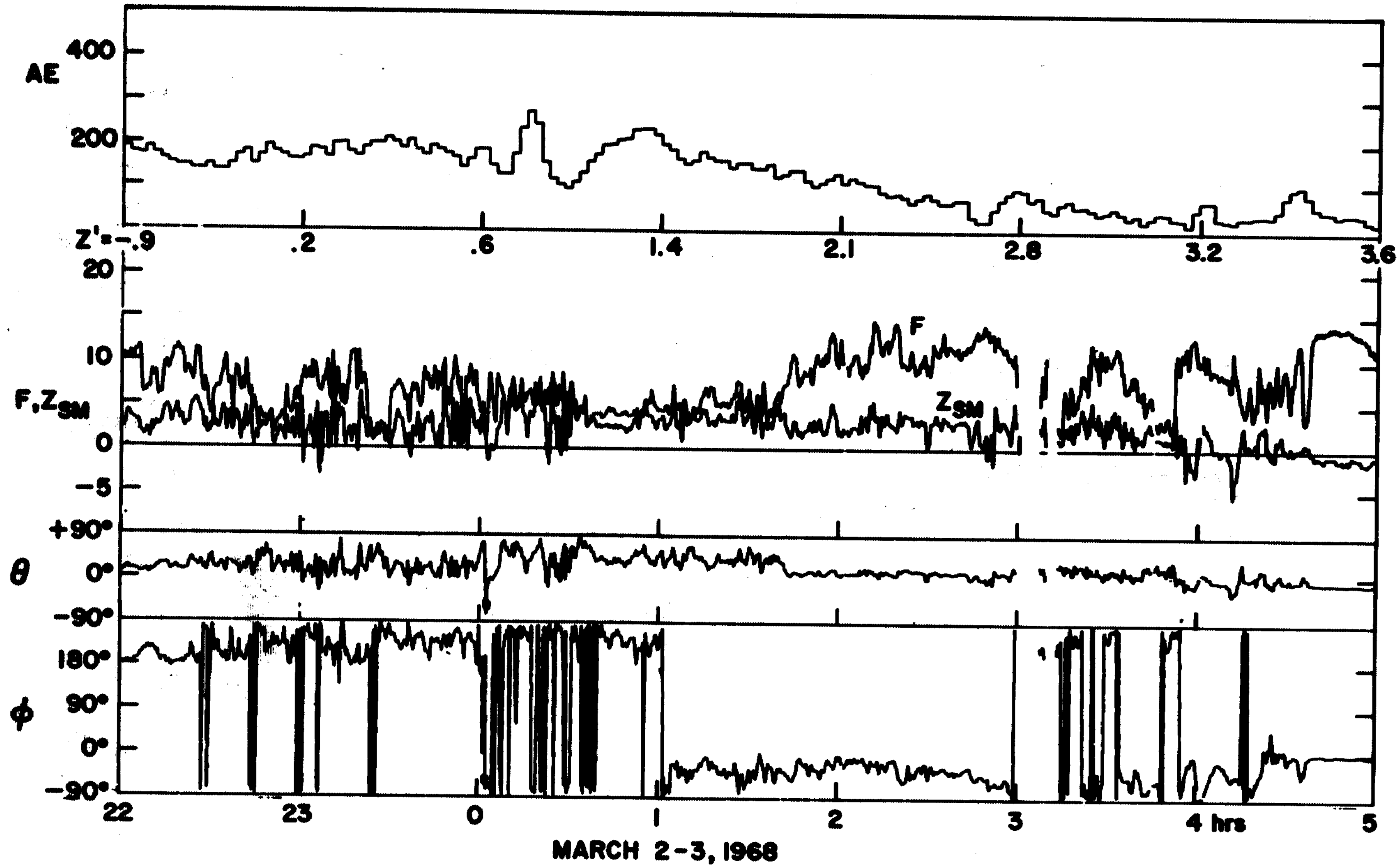
AE
400
200
Z'=-.9
.2
.6
1.4
2.1
2.8
3.2
3.6
20
10
F, Z_{SM}
0
-5
F
Z_{SM}
+90°
θ
0°
-90°
180°
φ
90°
0°
-90°
22
23
0
1
2
3
4 hrs
5
MARCH 2-3, 1968

FIGURE 8

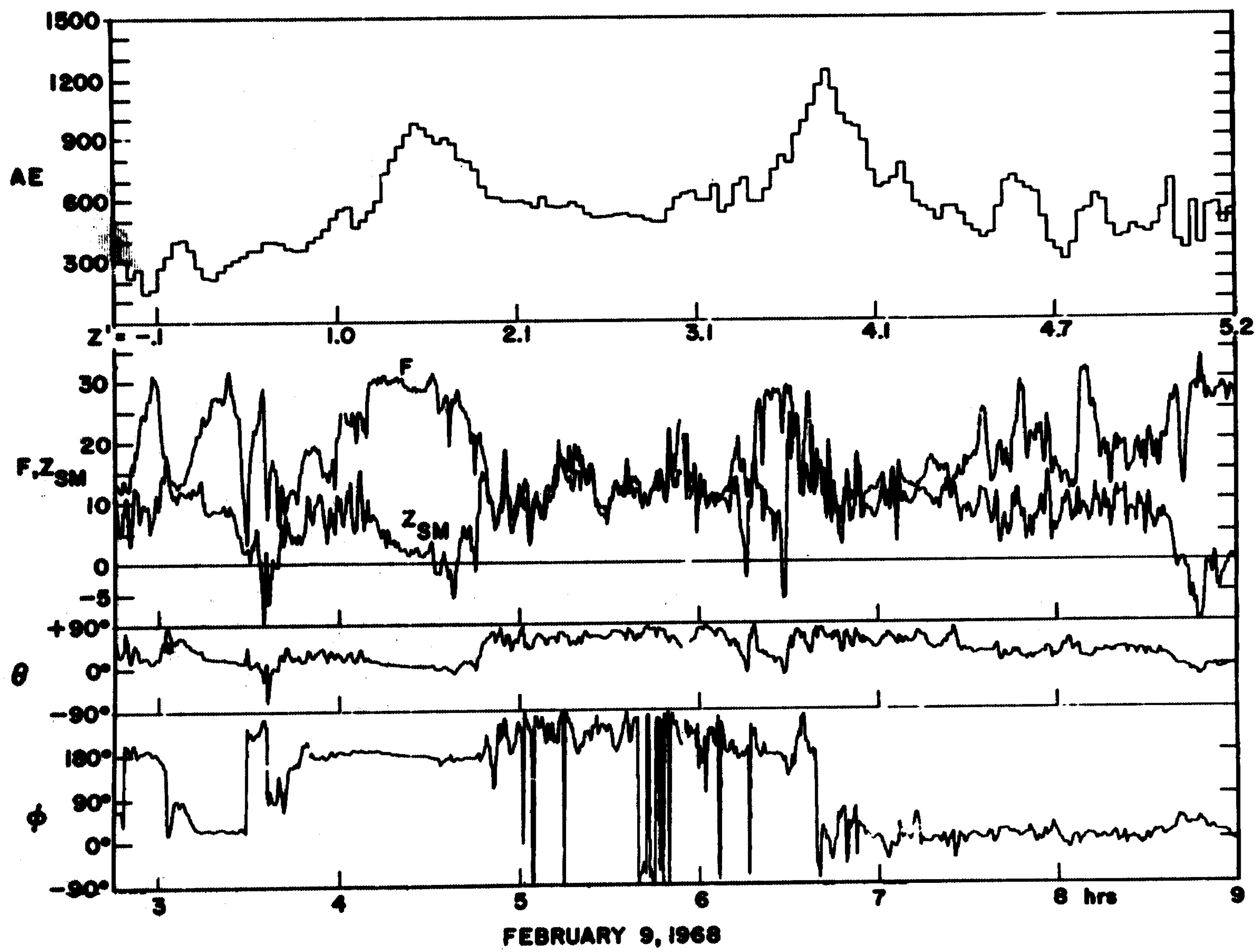

AE
1500
1200
900
600
300
Z' = -.1
1.0
2.1
3.1
4.1
4.7
5.2
F, Z_{SM}
F
Z_{SM}
30
20
10
0
-5
+90°
θ
0°
-90°
180°
φ
90°
0°
-90°
3
4
5
6
7
8 hrs
9
FEBRUARY 9, 1968

FIGURE 9

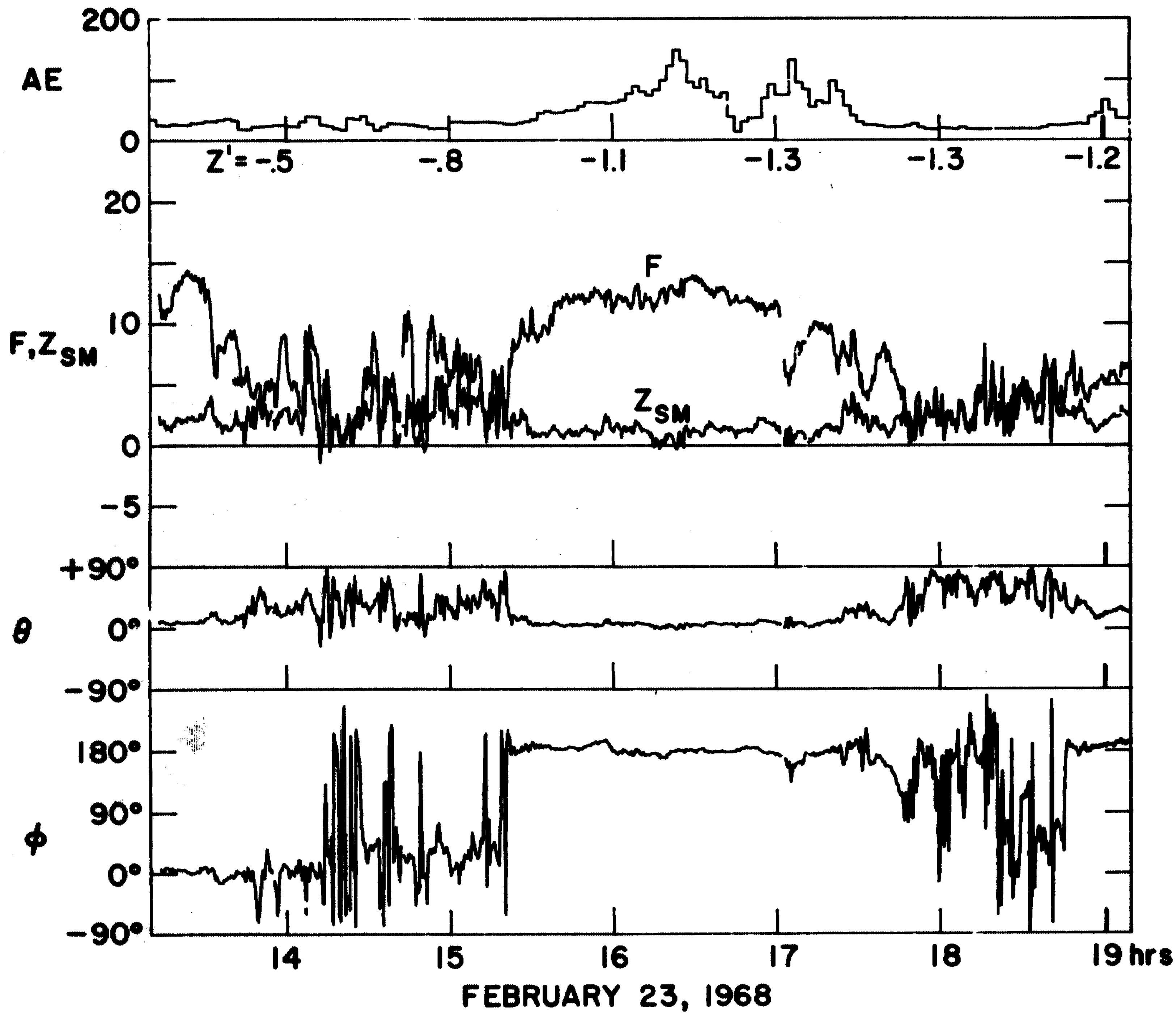
AE
200
0
Z' = -.5
-.8
-1.1
-1.3
-1.3
-1.2
20
F
F,Z_{SM}
10
Z_{SM}
0
-5
+90°
θ
0°
-90°
180°
φ
90°
0°
-90°
14
15
16
17
18
19 hrs
FEBRUARY 23, 1968

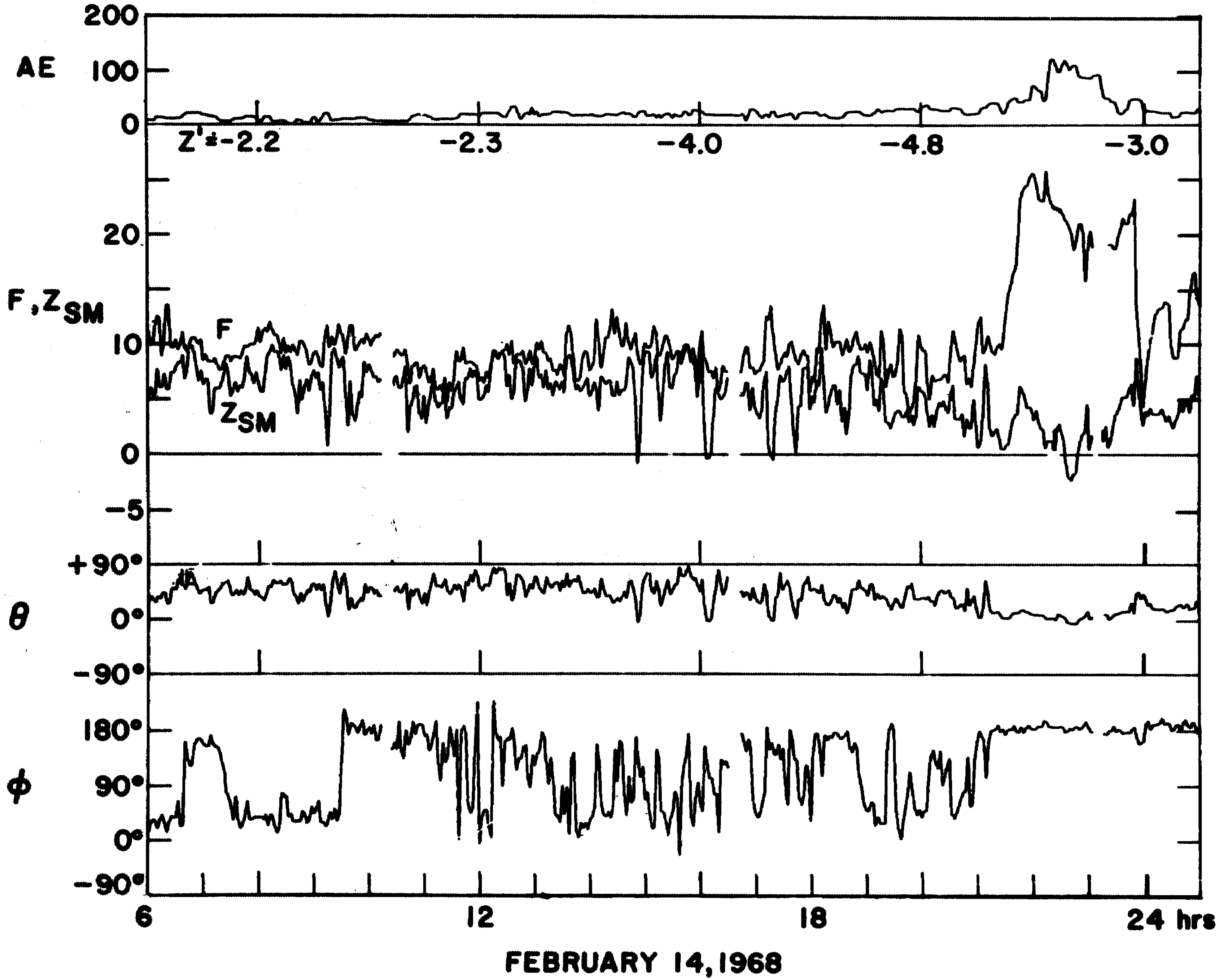

AE
200
100
0
Z'=-2.2
-2.3
-4.0
-4.8
-3.0
F, Z_{SM}
20
10
0
-5
F
Z_{SM}
θ
+90°
0°
-90°
φ
180°
90°
0°
-90°
6
12
18
24 hrs
FEBRUARY 14, 1968

FIGURE 11

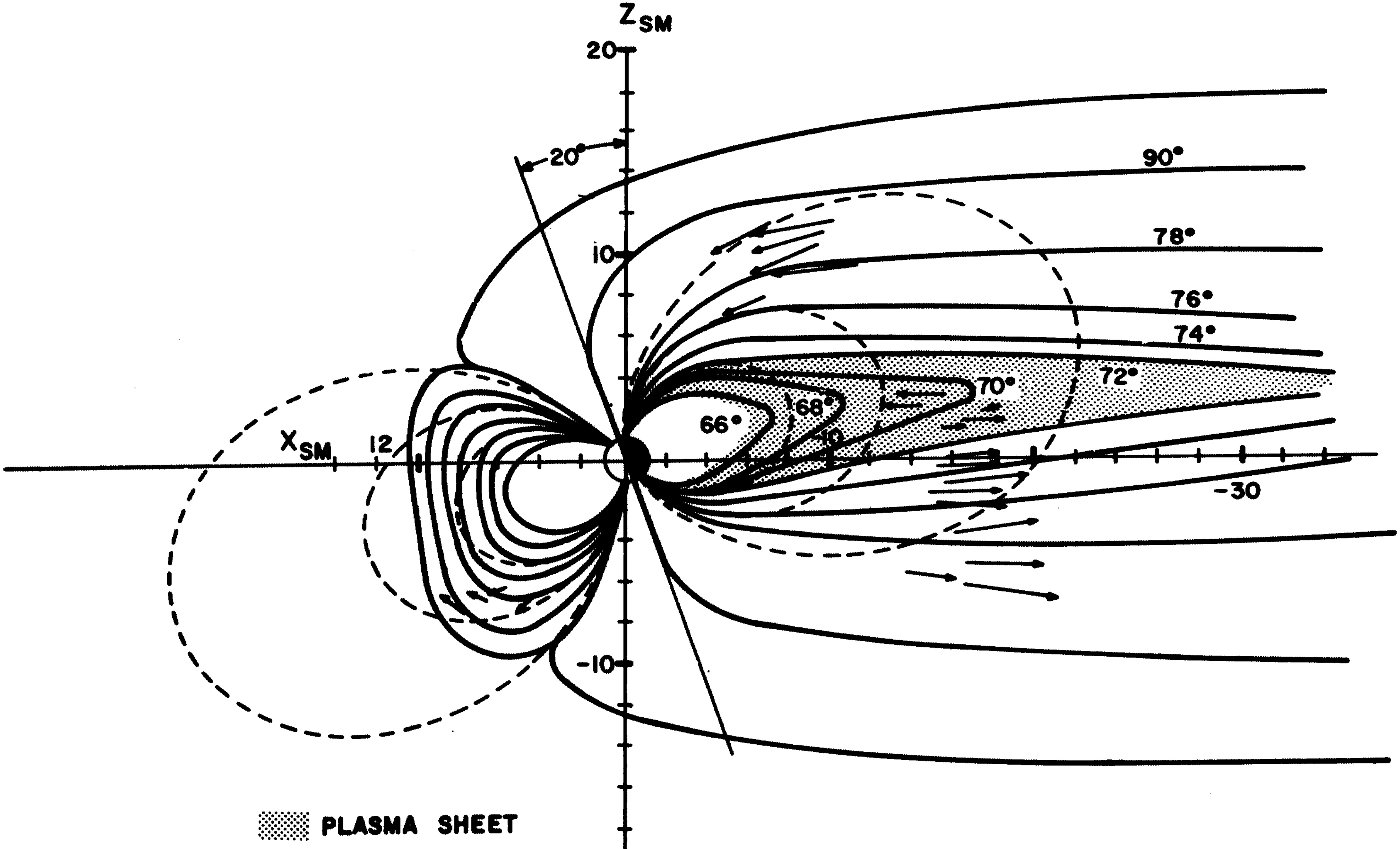

PRE-SUBSTORM MAGNETOSPHERE

FIGURE 12

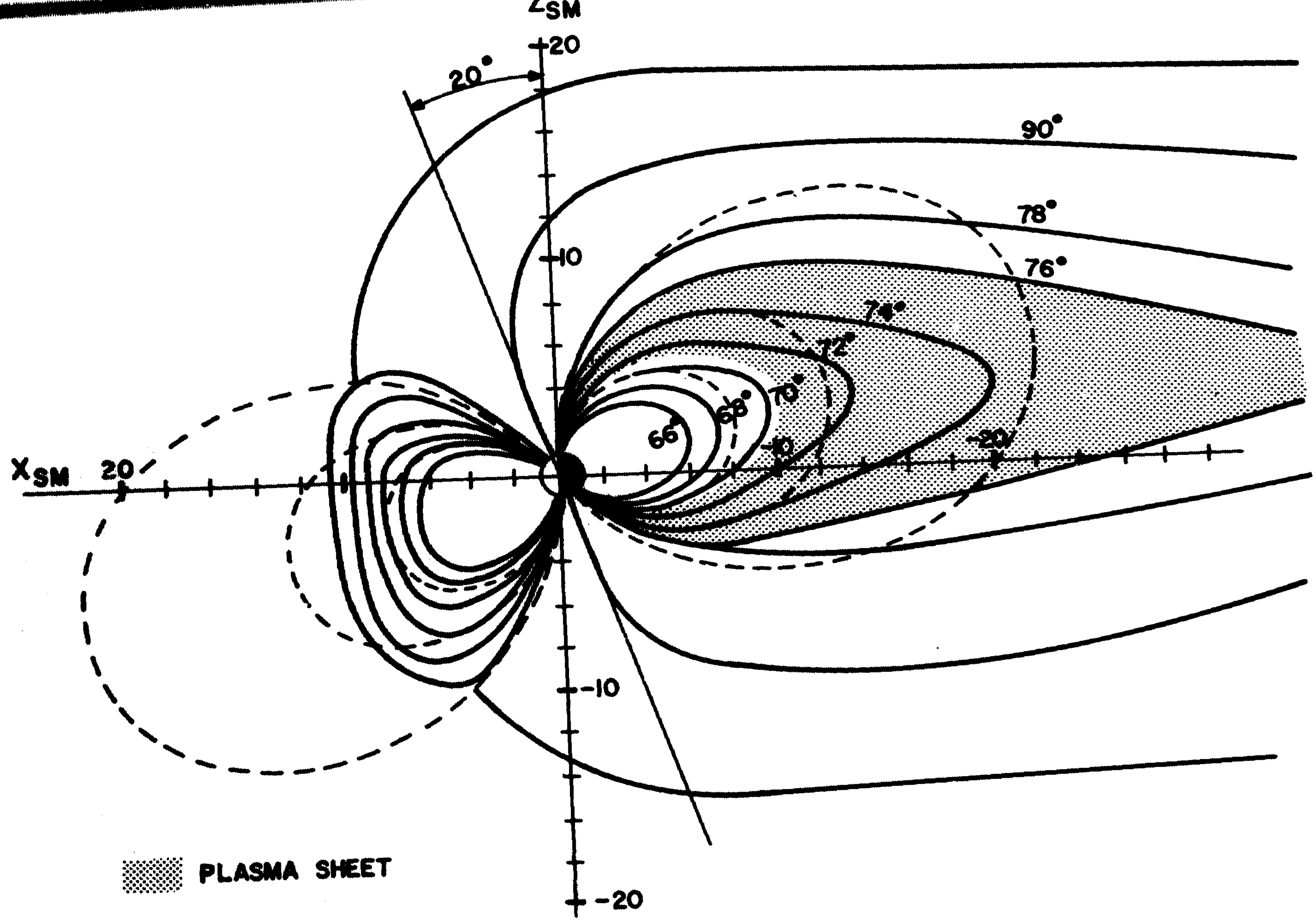

QUIET POST-SUBSTORM MAGNETOSPHERE

FIGURE 13